HHS Public Access

Author manuscript

Dev Biol. Author manuscript; available in PMC 2016 March 15.

Published in final edited form as:

Dev Biol. 2015 March 15; 399(2): 237–248. doi:10.1016/j.ydbio.2014.12.034.

Loss of *cftr* function leads to pancreatic destruction in larval zebrafish

Adam Navis[1] and **Michel Bagnat**[1]

Department of Cell Biology, Duke University Medical Center

Abstract

The development and function of many internal organs requires precisely regulated fluid secretion. A key regulator of vertebrate fluid secretion is an anion channel, the cystic fibrosis transmembrane conductance regulator (CFTR). Loss of CFTR function leads to defects in fluid transport and cystic fibrosis (CF), a complex disease characterized by a loss of fluid secretion and mucus buildup in many organs including the lungs, liver, and pancreas. Several animal models including mouse, ferret and pig have been generated to investigate the pathophysiology of CF. However, these models have limited accessibility to early processes in the development of CF and are not amenable for forward genetic or chemical screens. Here, we show that Cftr is expressed and localized to the apical membrane of the zebrafish pancreatic duct and that loss of *cftr* function leads to destruction of the exocrine pancreas and a cystic fibrosis phenotype that mirrors human disease. Our analyses reveal that the *cftr* mutant pancreas initially develops normally, then rapidly loses pancreatic tissue during larval life, reflecting pancreatic disease in CF. Altogether, we demonstrate that the *cftr* mutant zebrafish is a powerful new model for pancreatitis and pancreatic destruction in CF. This accessible model will allow more detailed investigation into the mechanisms that drive CF of the pancreas and facilitate development of new therapies to treat the disease.

Keywords

Cftr; cystic fibrosis; pancreas

Introduction

Fluid secretion is a key developmental process, required for the morphogenesis and function of many organs (Cartwright et al., 2009). During lumen formation, fluid secretion drives lumen coalescence and expansion in several organs including the gut, brain, and kidney (Bagnat et al., 2007; Kramer-Zucker et al., 2005; Lowery and Sive, 2005; Nedvetsky et al.,

Corresponding Author. Michel Bagnat, michel.bagnat@duke.edu, 333B Nanaline Duke Bldg., Box 3709, Duke University Medical Center, Durham, NC 27710, Telephone 919-681-9268.

Present Address

Adam Navis, Department of Chemical and Biological Engineering, Princeton University

2014). One of the key regulators of fluid secretion in several organs is the anion channel cystic fibrosis transmembrane conductance regulator (CFTR) (Bagnat et al., 2010; Navis et al., 2013; Nedvetsky et al., 2014). Loss of CFTR activity leads to CF, a multi-organ disease caused by defects in ion and fluid transport (Riordan et al., 1989). Mutations in CFTR can disrupt anion transport, leading to loss of chloride and/or bicarbonate transport necessary for regulating osmotic gradients that drive fluid secretion (Anderson et al., 1991; Barrett and Keely, 2000). Loss of CFTR activity in epithelia lining the tubular systems of affected organs allows mucus to accumulate within the lumen, blocking ducts and disrupting organ function (Durie and Forstner, 1989; Gaskin et al., 1988; Matsui et al., 1998). In the airways, mucus becomes compacted allowing invasion by opportunistic bacteria and leading to decline in lung function (Matsui et al., 1998). The thick mucus buildup characteristic of CF may be due to the loss of bicarbonate transport necessary for mucus expansion and fluidity (Quinton, 2008).

The pathology of CF was initially described as cystic fibrosis of the pancreas (Andersen, 1938). Loss of CFTR function in the pancreas leads to blockage of the pancreatic ducts with mucus and widespread destruction of acinar tissue, which is replaced by fibrotic tissue over time (Wilschanski and Novak, 2013). In most CF patients obstruction of the ductal system and destruction of the acinar tissue lead to pancreatic insufficiency (PI), characterized by impaired delivery of digestive enzymes to the intestine (DiMagno et al., 1973). Although the pathology of pancreatic disease in CF has been well characterized, the mechanisms leading to pancreatic destruction are less well understood.

Infant and fetal CF patients have high levels of circulating immunoreactive trypsinogen (Crossley et al., 1979), which is also a marker of pancreatitis in adults (Kemppainen et al., 1997). Further, pancreatic sufficient (PS) CF patients are susceptible to pancreatitis (Durno et al., 2002) and people carrying one defective CFTR allele have increased risk of developing chronic pancreatitis (Cohn et al., 1998; Sharer et al., 1998). Additionally, increased inflammatory cells, including neutrophils and macrophages, have been observed in the CF pancreas in humans and animal models (Andersen, 1938; Meyerholz et al., 2010; Olivier et al., 2012), however the mechanisms leading to widespread pancreatic destruction in CF remain poorly understood. The prevailing view of pancreatitis onset is that ductal blockage leads to activation of digestive enzymes within the acinar tissue, leading to auto-digestion, then inflammation and recruitment of the innate immune system (Lerch and Gorelick, 2013; Whitcomb, 2004). However, a recent study has challenged this model of disease onset and suggested that inflammation driven by neutrophils is a major driver of zymogen activation and auto-digestion of acinar tissue (Sendler et al., 2013). Identifying the precise sequence of events leading to pancreatic disease in CF patients will be essential to better understand the pathophysiology of CF.

To investigate the pathophysiology of CF several animal models have been developed including the mouse, pig, and ferret (Dorin et al., 1992; Rogers et al., 2008; Snouwaert et al., 1992; Sun et al., 2010). Mouse models develop intestinal obstruction similar to CF patients (Hodges et al., 2011), but fail to develop spontaneous lung disease and present only mild disease in the pancreas, which can take many months to become apparent (Durie et al.,

2004), likely due to compensatory calcium activated chloride channels (Rock et al., 2009; Snouwaert et al., 1992).

To address the lack of lung disease in the mouse model, ferret and pig models of CF were generated by disrupting *CFTR* in these systems (Rogers et al., 2008; Sun et al., 2008). The pig and ferret models develop the pathophysiology characteristic of CF in many organs including lung dysfunction and severe pancreatic destruction (Rogers et al., 2008; Sun et al., 2010). Although these models have led to new insights into the pathophysiology of CF, the limited accessibility of developmental stages, high animal husbandry costs, and the impracticality of genetic analyses in these systems hinders their widespread use. To better understand disease onset and to develop new treatments for CF, it will be essential to develop a more accessible model of CF that reflects the severity of human disease. The zebrafish is a powerful genetic model system, which has been used to model several human diseases (Phillips and Westerfield, 2014). Zebrafish Cftr is similar to human CFTR and is responsive to many of the same pharmacological activators and inhibitors of human CFTR activity (Bagnat et al., 2010). Previously, we showed that *cftr* is necessary for fluid secretion and lumen expansion of Kupffer's vesicle, an organ controlling laterality during early zebrafish development, highlighting the role of *cftr* during the regulation of fluid secretion in the zebrafish (Navis et al., 2013). Since *cftr* regulates fluid secretion early in development, we hypothesized that *cftr* may also be essential for organogenesis and organ function later in life, similar to mammalian CFTR.

Here, we describe a zebrafish model of pancreatic disease in CF. We found that Cftr is expressed in the pancreatic duct and localized to the apical membrane throughout the life, similar to mammalian expression. We further examined the role of *cftr* in the pancreas, finding that exocrine pancreatic destruction develops rapidly at around two weeks post fertilization. Importantly, we found that the *cftr* mutant zebrafish develops pancreatic destruction similar to CF of the human pancreas.

Materials and Methods

Fish stocks

Zebrafish were maintained at 28°C and propagated as previously described (Westerfield, 2000). The *cftr*^{pd1049} mutant line was maintained in the AB background (Navis et al., 2013). Homozygous *cftr*^{pd1049} mutant fish were identified by sorting zebrafish at 10–12 somite stage for loss of Kupffer's vesicle lumen inflation (Navis et al., 2013). After fertilization, the fish were raised at 24°C overnight to better schedule the optimal sorting period. Once sorted, the zebrafish were maintained at 28°C. Zebrafish care and maintenance was performed in accordance with the Duke Institutional Animal Care and Use Committee. The following transgenic zebrafish lines were used in this study: EK, AB, *TgBAC(cftr-GFP)pd1041, TgBAC(cftr-RFP)pd1042, Tg(ptf1a:GFP)jh1* (Godinho et al., 2005), *TgBAC(ptf1a:Gal4)jh16* (Parsons et al., 2009), *TgBAC(cftr:Gal4)pd1101* (this study), *Tg(UAS:GFP)zf82* (Asakawa et al., 2008), *Tg(UAS:mCherry*), *Tg(ela:GFP, lfabp:dsRed)gz12* (Farooq et al., 2008), *Tg(lysC:dsRed)nz50* (Hall et al., 2007) and *Tg(ins:dsRed)m1018* (from W. Driever, Freiburg, Germany).

In situ hybridization

In situ hybridization was performed as previously described with slight modifications (Navis et al., 2013; Snelson et al., 2008). Briefly, AB zebrafish were fixed in 4% paraformaldehyde overnight. Fixed fish at 3 and 5 dpf were treated with 10 μg/ml Proteinase K (Sigma, St. Louis, MO, USA) for 20 min prior to hybridization. After staining, the fish were dehydrated in a glycerol series to clear and imaged on a Discovery V20 stereoscope (Zeiss) in 100% glycerol.

BAC recombineering

Bacterial artificial chromosome (BAC) recombineering was used to generate the *TgBAC(cftr:Gal4)pd1101* line using the SW105 cell line with slight modifications to a previously described protocol (Warming et al., 2005). A selection cassette containing Gal4-VP16 followed by an FRT flanked Kanamycin resistance gene was assembled in pBluescript. The SW105 cells were transformed with the *cftr* BAC. The Gal4 FRT-Kan-FRT cassette was then amplified using primers containing 50 bp of homology to the sequences flanking the *cftr* start codon: *cftr*-gal4-F, GATACCCGTAACCCGATGTGAGCGCTTTCACCCCCGGGGTACTTTTTAGGATGAAGCTACTGTCTTCTAT and *cftr*-gal4-R, CAAAAGAAGTATCTGGAGAGGCAGTTGGCATCCTCCACAGGTGATCTCTGCAGTGTGATGGATATCTGCAG. SW105 cells containing the *cftr* BAC were induced by heatshock then transformed with this PCR product and selected using kanamycin. The kanamycin selection cassette was removed by arabinose induction of the Flpase expressed in the SW105 cells. Finally, the *cftr:Gal4* BAC was further recombined with iTol2-Amp (Suster et al., 2009) to deliver inverted Tol2 sites to the BAC vector sequence using the following primers: iTol2-indigo-F, TCTCTGTTTTTGTCCGTGGAATGAACAATGGAAGTCCGAGCTCATCGCTACCCTGCTCGAGCCGGGCCCAAGTG and iTol2-indigo-R, CGACACCCGCCAACACCCGCTGACGCGAACCCCTTGCGGCCGCATCGAATATTATGATCCTCTAGATCAGATCT. The completed *cftr:Gal4* BAC DNA was prepared using the Nucleobond BAC-100 kit (Clontech, Mountain View, CA, USA). Zebrafish were injected with 75 pg BAC DNA and 50 pg transposase RNA. Fish were screened for transgenesis by mating to the *Tg(UAS:GFP)zf82* line to drive GFP expression and a line with robust *UAS:GFP* induction was selected to generate the *TgBAC(cftr:Gal4)* line.

Live imaging

Live imaging was performed by mounting fish anesthetized with 0.16 mg/ml tricaine (Sigma, A5040) in 3% methylcellulose. Pancreatic ducts expressing Cftr-GFP or Cftr-RFP were imaged using an upright Leica SP5 confocal microscope using a 40× HCX PL APO objective. Stacks of z-planes from the pancreatic ducts were compiled using Fluorender to generate three dimensional reconstructions (Wan et al., 2012). Larvae for quantification of secondary islets were similarly prepared and imaged using a Zeiss Imager M1 with an EC Plan-Neufluar 10×/0.3 objective.

Immunofluorescence

Antibody staining of wholemount zebrafish was performed as previously described (Dong et al., 2007). Briefly, larvae were fixed with 3% formaldehyde (Mallinkrodt) in 0.1 M PIPES (Sigma), 1.0 mM MgSO4 (Sigma), and 2 mM EGTA (Sigma) at pH 7.0 (PEM solution) overnight at 4°C. The ventral skin flanking the liver and pancreas was removed with forceps and any remaining yolk was removed. The larvae were then stained with anti-insulin (Dako, Carpinteria, CA, USA, 1/100, guinea pig), anti-glucagon (Sigma, 1/200, mouse), or anticarboxypeptidase (anti-CP-A) (Rockland, Philadelphia, PA, USA, 1/500, rabbit). Primary antibodies were detected using goat anti-mouse Alexa488 (Molecular Probes, Grand Island, NY, USA, 1/300), goat anti-guinea pig Alexa568 (Molecular Probes, 1/300), or goat anti-rabbit Alexa568 (Molecular Probes, 1/300) in addition to either Alexa Fluor 568 or 647 Phalloidin (Molecular Probes, 1/500) to mark filamentous actin. Stained wholemount zebrafish were dehydrated in a glycerol series and mounted in 100% glycerol for imaging.

Zebrafish sections were prepared for immunofluorescence and confocal microscopy as previously described (Alvers et al., 2014; Bagnat et al., 2007). Whole larvae and adult visceral organs were removed by dissection and were placed in 3% formaldehyde in PEM. Samples were mounted in 4% low melt agarose (Bioline, Kaysville, UT, USA) and cooled at 4°C for at least 1 hour. The resulting blocks were sectioned using a Leica VT 1000S Vibratome to generate 200 μm (larvae) to 300 μm (adult) sections. These sections were stained with anti-carboxypeptidase (Rockland, 1/500, rabbit), anti-insulin (Dako, 1/100, guinea pig), anti-glucagon (Sigma, 1/200, mouse), or zn-5 (Zebrafish International Research Center, 1/1000, mouse). The primary antibodies were detected as above. Samples were imaged using a Leica SP5 confocal microscope.

Histology

The visceral organs from adult zebrafish were removed by dissection and immediately placed in 4% PFA for 48 hours at 4°C. Histology was performed as previously described (Moss et al., 2009). Periodic Acid Schiff (Sigma, 395B) was performed on paraffin sections according to the manufacturer's suggestions. Stained sections were imaged with a Zeiss Discovery.V20 stereoscope using a PlanApo S 3.5× mono objective.

Pharmacological treatments

Precocious secondary islets were induced by treatment with DAPT (Sigma, D5942). Fish were treated with 100 μM DAPT or DMSO in egg water from 3 to 5 dpf and secondary islets were analyzed at 7 dpf (Parsons et al., 2009). To disrupt neutrophil recruitment, zebrafish larvae were treated with 0.5 μM PF1052 (Wang et al., 2014) (Enzo Life Sciences, Farmingdale, NY, USA, ALX-380-147) from 14 to 18 dpf. Fish were placed in 0.5 μM PF1052 or 0.005% DMSO in egg water at 14 dpf. The fish were transferred to new water at 16 dpf and the fish were fed overnight at 15 and 17 dpf. Treated fish were fixed overnight at 4°C in 3% formaldehyde in PEM solution at 18 dpf. Fixed larvae were sectioned and imaged as above.

Statistical Analysis

Total number of β cells was determined by obtaining confocal stacks through complete islets. The β cells of principal islets were visualized using an anti-insulin antibody (Dako, 1/100). Secondary islet β cells were visualized using the *Tg(ins:dsRed)* transgenic line on a Zeiss Imager M1 with a EC Plan-Neufluar 10×/0.3 objective. Total number of β cells and secondary islets were compared between *cftr* mutants and their WT siblings using a two tail unpaired Student's t-test.

The relative acinar area of transverse sections of WT and *cftr* mutant pancreata expressing *ela:GFP* was compared using ImageJ (NIH, Bethesda, MD, USA). The area of *ela:GFP*-expression was obtained using ImageJ to threshold and segment the GFP expressing pixels. The total area of the pancreas was obtained by outlining the pancreas using the polygon selection tool. The relative GFP area for each sample was determined by dividing the *ela:GFP*-expressing area by total pancreas area for each sample and the vehicle versus PF1052 treatment groups were compared using a two tail unpaired Student's t-test.

Neutrophil recruitment to the pancreas was quantified by analyzing whether neutrophils were present in pancreatic sections from WT and *cftr* mutant samples. We grouped samples by the presence or absence of neutrophils in the pancreas. The total number of samples in each group was summed and compared using the chi-squared test. We also plotted the average number of neutrophils observed in each pancreas and compared the two groups using a two tail unpaired Student’s t-test.

Body length was determined at various ages using ImageJ. Fish were anesthetized with tricaine, then imaged with a standard length reference. The body lengths were determined using the line tool in ImageJ to trace the distance from the tip of the mouth to the end of the tail. The average body lengths for each group were compared using a two tail unpaired Student's t-test.

Survival was tracked for 30 WT and 30 *cftr* mutant siblings from day 7 to day 32. At each timepoint, the total number of fish remaining in each group were counted. The relative survival was plotted against the total time of the experiment.

Results

Expression and localization of Cftr

In the pancreas of humans and other mammals, CFTR is expressed primarily within the pancreatic ducts (Cohn et al., 1993; Ostedgaard et al., 2011). To determine whether the mammalian CFTR expression pattern is reflected in the zebrafish we first investigated the *cftr* expression pattern. Using in situ hybridization to detect the *cftr* transcript, we found that *cftr* is expressed in the pancreas at 3 days post fertilization (dpf). This corresponds to an early stage in the development of the pancreatic duct, as the ductal network is forming from unpolarized progenitors and its expression pattern is similar to other markers of the developing pancreatic duct (Pauls et al., 2007; Yee et al., 2005) (Fig. 1A,B). At 5 dpf, *cftr* was detected in a branched pattern reflecting the morphology of the pancreatic duct at later stages (Fig. 1C,D).

To observe the dynamics of Cftr expression and localization of in the zebrafish pancreas more closely, we utilized a pair of BAC transgenic lines encoding functional C-terminal Cftr-GFP or Cftr-RFP fusion proteins (Navis et al., 2013). We first examined expression of *TgBAC(cftr-GFP)* at 3 dpf, during the initial stages of pancreatic duct development. At this stage, Cftr-GFP is expressed in the center of the pancreas, distinctly from the expression pattern of *TgBAC(ptf1a:Gal4)* in the acinar cells and consistent with expression of *cftr* in the pancreatic duct (Fig. 1E). In transverse section at 5 dpf, Cftr-GFP remained in the center of the pancreas, indicative of expression within the pancreatic duct (Fig. 1F).

To determine whether *cftr* is expressed along the length of the pancreatic duct, we performed live confocal imaging of 6 dpf pancreata in the sagittal plane. Cftr expression from T*gBAC(cftr-GFP)* was visualized in conjunction with *Tg(ins:dsRed)* to mark the β cells of the pancreatic islet. We found that Cftr-GFP is localized along the pancreatic duct in a pattern distinct from the endocrine cells of the principal islet (Fig. 1G, supplementary material Movie 1). Although *cftr* expression has been reported at low levels in the β cells of the islets in other systems (Boom et al., 2007; Guo et al., 2014), we did not observe *cftr* expression in the islets, which may be expressed below visual detection limits. To examine expression of *cftr* in conjunction with the cells of the acinar cells of the exocrine pancreas, we imaged *TgBAC(cftr-RFP)* in the *Tg(ela:GFP, lfabp:dsRed)* background at 6 dpf, which expresses GFP in the pancreatic acinar cells and dsRed in the liver. Live confocal imaging of these fish revealed that *cftr* is expressed in a thin stripe in the center of the pancreas, indicative of ductal localization (Fig. 1H, supplementary material Movie 2). These results demonstrate that *cftr* is expressed along the pancreatic duct in zebrafish.

We next investigated the localization of Cftr within the pancreatic duct epithelium. The *TgBAC(cftr-GFP)* and *TgBAC(cftr-RFP)* lines, which express full length GFP or RFP-tagged Cftr were previously shown to localize apically within the polarized Kupffer's vesicle epithelium (Navis et al., 2013). To determine whether Cftr is also localized at the apical membrane in the pancreatic duct, we wanted to visualize Cftr localization in conjunction with a specific, cytosolic marker of the pancreatic duct epithelium. To this end we generated a new transgenic line using the *cftr* BAC to drive Gal4-VP16 expression (*TgBAC(cftr:Gal4)*). To examine the intracellular localization of Cftr within the cells where it is normally expressed, we generated zebrafish expressing *TgBAC(cftr-RFP); TgBAC(cftr:Gal4); Tg(UAS:GFP)*. In these fish, the cytoplasm of the pancreatic duct epithelium is labeled by GFP, and Cftr-RFP can be clearly seen localized to the apical membrane of opposing cells lining the lumen of the pancreatic duct (Fig. 2A,A'). Additionally, we detected high levels of *cftr* expression in discrete cells along the intestinal epithelium (Fig. 2A,A'), similar to what was previously reported in mammals using immunohistochemistry (Ameen et al., 1995). As in mammalian systems, Cftr-RFP was localized to puncta near the apical surface, where it may help regulate intestinal fluid secretion (Fig. 2A,A').

We also examined Cftr localization at later stages in fish expressing *TgBAC(cftr-RFP)* in the pancreatic duct and *ptf1a:GFP* expressed in the surrounding acinar tissue. To mark the apical membrane of the pancreatic duct, we used phalloidin to detect filamentous actin, which is a well-characterized marker of the apical membrane of the pancreatic duct (Fallon

et al., 1995; Kesavan et al., 2009). At 21 dpf, Cftr-RFP was localized at or near the apical membrane of the ductal cells, marked by phalloidin staining, and did not overlap with the acinar marker *ptf1a:GFP* (Fig. 2B,B'). We also examined expression of *cftr* in the adult zebrafish, and found Cftr-GFP localized in a similar pattern as phalloidin in the adult pancreatic duct, indicating that Cftr is a clear marker of the apical membrane of the pancreatic duct in the adult zebrafish pancreas (Fig. 2C,C',D,D'), similar to previous descriptions of the human pancreas (Cohn et al., 1993). These results reveal that *cftr* is a robust marker of the pancreatic duct from its formation and throughout zebrafish life.

Pancreatic development is not affected in *cftr* mutants

Since *cftr* is expressed in the early stages of pancreatic development, we next investigated whether *cftr* mutants have defects in the development of the pancreas. We tested whether loss of *cftr* function leads to defects in lumen formation in the pancreatic duct, which may underlie ductal blockages seen later in life. Consistent with this hypothesis, fluid secretion has been previously shown to be important for single lumen formation in the zebrafish intestine (Bagnat et al., 2007) and lumen opening in Kupffer's vesicle (KV) (Navis et al., 2013). One possibility is that loss of Cftr-dependent fluid secretion may lead to defects in lumen formation in the pancreatic duct. In WT zebrafish, the pancreatic duct extends along the length of the pancreas at 5 dpf, marked by apical accumulation of filamentous actin (Fallon et al., 1995; Kesavan et al., 2009). We examined *cftr* mutants for discontinuous filamentous actin, which would be indicative of defects in the formation of a continuous ductal lumen. We found no differences in the formation of the pancreatic duct between *cftr* mutant and WT larvae, indicating that the pancreatic duct undergoes successful lumen formation (Fig. 3A,A',B,B').

We next examined whether *cftr* mutants have defects in the development of the exocrine pancreas. To determine whether the pancreas has any defects in gross morphology we examined 5 and 10 dpf larvae expressing *Tg(ela:GFP)* to label acinar cells. We found that in *cftr* mutant fish the acinar tissue appears identical to WT siblings at 5 and 10 dpf (Fig. 3C–F), indicating that the exocrine pancreas also develops normally during the initial stages of larval development in *cftr* mutant zebrafish.

Many CF patients with pancreatic insufficiency also develop cystic fibrosis related diabetes (CFRD), which may be due to defects in the function or composition of pancreatic islets (Mackie et al., 2003). We therefore examined whether defects in the development of β cells underlie the changes seen CFRD. The zebrafish islet contains two types of islets, the principal islet, which is specified early in pancreatic development, and the secondary islets, which arise later through a process more similar to the formation of mammalian islets (Parsons et al., 2009). The total number of β cells in the principal islet was similar between *cftr* mutants and their WT siblings at several stages from 3 to 14 dpf (Fig. 3G). We next examined the total number of secondary islets at 14 dpf and found that *cftr* mutants contained similar numbers of secondary islets and similar total number of β cells within those islets compared to their WT siblings (Fig. 3H,I). Even at 14 dpf, secondary islets are relatively rare, so we stimulated precocious islet formation by treating with DAPT, a previously characterized inhibitor of gamma secretase activity that induces early secondary

islet formation (Parsons et al., 2009). After treatment with DAPT, we again observed that the total number of secondary islets and β cells remained similar between *cftr* mutants and their WT siblings at 7 dpf (Fig. 3J,K). Together, these results indicate that the initial development of β cells occurs normally in *cftr* mutant zebrafish.

Additionally, we also examined maternal-zygotic *cftr* mutants and found no gross developmental abnormalities in the pancreas except for the previously reported situs defect that stems from the loss of KV function (Navis et al., 2013). Altogether, these results indicate that pancreatic organogenesis occurs normally during the early stages of development in *cftr* mutant zebrafish.

Pancreatic destruction in *cftr* mutants

To determine whether *cftr* is instead required for pancreatic function in the larval zebrafish, we next examined later stages to identify whether *cftr* mutant zebrafish undergo pancreatic destruction similar to CF. While raising *cftr* mutants to adulthood, we observed that a large percentage of the mutants are lost beginning around 10 dpf (supplementary material Fig. S1A). Furthermore, we noted that the *cftr* mutants begin to experience growth restriction coincident with the decreased survival (supplementary material Fig. S1B), suggesting that pancreatic defects may begin around this stage. At 12 dpf, the acinar tissue appears similar between WT and *cftr* mutant siblings (Fig. 4A,B). At 14 dpf, the acini of WT and *cftr* mutant siblings again appear largely similar (Fig. 4C,D), but some mild disruption can be detected in the *cftr* mutant pancreas. By 16 dpf, loss of acinar tissue is readily apparent, with a large amount of tissue lost in every *cftr* mutant zebrafish we examined at this stage (Fig. 4E,F). At 22 dpf, most pancreatic acinar tissue is absent in the *cftr* mutant fish (Fig. 4G,H). This progression is indicative of pancreatic destruction beginning between 14 and 16 dpf. The loss of *ela:GFP* marked tissue is similar to the pattern observed in adults, with a thin layer of remaining acinar cells surrounding a core of disrupted tissue. The rapid and widespread loss of pancreatic tissue appears highly similar to the destruction observed in mammalian models of CF, indicating that the zebrafish models severe pancreatic disease in CF.

Pancreatic destruction in adult *cftr* mutant zebrafish

In the majority of CF patients, the acinar tissue in the exocrine pancreas undergoes severe destruction and is largely replaced by fibrotic tissue (Wilschanski and Novak, 2013). To determine whether *cftr* mutant zebrafish develop the hallmarks of pancreatic disease characteristic of CF patients, we next examined the adult zebrafish pancreas. We first assessed the integrity of the exocrine pancreas by examining expression of a transgenic line that expresses GFP in the acinar cells and dsRed in the liver (*Tg(ela:GFP; lfabp:dsRed*). In WT zebrafish, *ela:GFP* expression can be widely observed throughout the pancreas; however, in *cftr* mutant siblings, the *ela:GFP* expression is restricted to the periphery of the pancreas and appears to be replaced by actin-rich, fibrotic tissue (Fig. 5A,B). The loss of pancreatic acini is consistent with severe pancreatic disease observed in human patients and other mammalian models.

In contrast to the severe destruction of exocrine tissue, the endocrine islets are largely spared in human patients, but they appear more disorganized due to a change in the composition of the islets (Iannucci et al., 1984; Löhr et al., 1989). Additionally, the β cells of the CF pancreas have reduced function, displaying altered responses to blood glucose (Handwerger et al., 1969; Olivier et al., 2012). We examined the composition of the zebrafish islets by staining for α and β cells in the islets. In contrast to the large core of β cells surrounded by a layer of α cells present in WT fish at 3 months post fertilization, the islets of the *cftr* mutant pancreas seem disorganized, appearing smaller and more numerous than those of their WT siblings (Fig. 5C,D).

We also examined the histology of the adult zebrafish pancreas using hemotoxylin and eosin staining of pancreata from 3 months post fertilization WT and *cftr* mutant siblings. We found that mutants undergo severe pancreatic destruction in a pattern highly reminiscent of the human CF pancreas (Fig. 5E,F). At this stage, the *cftr* mutant pancreas contains small groups of remaining acinar tissue interspersed between large amounts of fibrotic tissue. To determine whether the exocrine pancreas is further lost in older zebrafish, we examined one year old *cftr* mutants and found that the characteristic composition of acinar tissue is almost completely absent, with surviving acinar tissue restricted to the periphery of the pancreas (Fig. 5G,H). Close observation revealed that in *cftr* mutants the acinar tissue appeared to be replaced by a large amount of fibrotic tissue surrounding dilated ducts and islets that are largely spared from the surrounding destruction. This is similar to CF in human and in mammalian animal models, where the pancreatic ducts become filled and dilated by a large amount of mucus (Andersen, 1938; Rogers et al., 2008; Sturgess, 1984; Sun et al., 2010). To determine whether the zebrafish ducts are similarly filled with mucus, we performed Periodic Acid Schiff (PAS) staining on adult pancreatic sections. PAS staining detected that the dilated ducts in *cftr* mutant zebrafish are also filled with mucus (Fig. 5I,J). Altogether, these results indicate that the *cftr* mutant zebrafish pancreas develops severe pancreatic disease mirroring that of human CF patients.

Immune response and pancreatic destruction

We next investigated the role of neutrophils during pancreatic destruction in *cftr* mutants. Neutrophils and other members of the innate immune response have previously been detected in the CF pancreas, though their precise role during pancreatic destruction is unknown (Abu-El-Haija et al., 2012; Andersen, 1938; Meyerholz et al., 2010; Olivier et al., 2012). A hallmark of pancreatitis is neutrophil infiltration, which occurs early during pancreatitis (Mayerle et al., 2005). We therefore examined whether neutrophils are similarly recruited to the pancreas in *cftr* mutants during the early stages of pancreatic destruction by examining a transgenic line expressing dsRed in neutrophils (*Tg(lysC:dsRed)*) (Hall et al., 2007; Yang et al., 2012). We crossed this line into the $cftr^{pd1049}$ background and examined *cftr* mutants and WT siblings at several stages. At 14 dpf, we did not observe neutrophils in the pancreas of *cftr* mutants or their WT siblings (Fig. 6A,B). However, at 16 dpf, neutrophils were more frequently detected in the *cftr* mutant pancreas than in WT, at a stage when pancreatic destruction is apparent (Fig. 6C–F).

The prevailing view of pancreatitis suggests that ductal blockage leads to activation of zymogens trapped within the acinar cells. This in turn leads to digestion of the acinar tissue, causing tissue damage, inflammation, and neutrophil recruitment. The neutrophils then amplify the inflammatory signal, eventually leading to replacement with fibrotic tissue (Lerch and Gorelick, 2013; Whitcomb, 2004). However, a recent report suggests that neutrophils may instead play a more central role in the process of auto-digestion. In this alternative model, neutrophils are recruited early and generate inflammatory signals that cause the acinar cells to drive activation of intracellular zymogens (Sendler et al., 2013).

We next used a recently described inhibitor of neutrophil migration, PF1052 (Wang et al., 2014), to examine the role of neutrophils during pancreatic destruction. WT and *cftr* mutant siblings were treated from 14 to 18 dpf with 0.5 μM PF1052. This treatment had no obvious effects on WT larvae which appeared to be healthy, and the PF1052 treated WT pancreata were indistinguishable from vehicle-treated controls (Fig. 6G,I). In contrast, *cftr* mutant zebrafish treated with PF1052 demonstrated a significant preservation of acinar tissue compared to vehicle treated mutants (Fig. 6H,J,K). PF1052 did not completely rescue the amount of acinar tissue to WT levels, likely due to a lower dose of PF1052 than previous reports (Wang et al., 2014), which may incompletely block migration. PF1052 at the higher, previously published dose was toxic for overnight treatment. These data suggest that neutrophils play a role in acinar destruction in the zebrafish pancreas.

Discussion

In this study we describe a new zebrafish model of CF, which recapitulates many aspects of the pancreatic disease observed in humans. Lacking *cftr* activity, the zebrafish pancreatic ducts are filled with mucus and the pancreatic acinar tissue is rapidly destroyed. We also found that the zebrafish had no major defects in the initial development of the pancreas, indicating that pancreatic destruction occurs due to processes that take place after the pancreas is formed. Interestingly, the destruction is accompanied by a modest but significant increase in neutrophil infiltration, in a process that appears similar to the onset of pancreatitis.

In zebrafish mutant for *cftr*, pancreatic destruction begins between 14 and 16 dpf, leading to rapid destruction of acinar tissue. The *cftr* mutant zebrafish pancreas displays several hallmarks of pancreatitis including recruitment of neutrophils to the affected area, destruction, and later replacement of the affected tissue by fibrosis. These changes are reminiscent of CF in the pancreas and demonstrate that *cftr* function in the zebrafish is similar to that in mammals.

Traditionally, neutrophils have been thought to be recruited after the acinar cells begin to be digested (Whitcomb, 2004); however, a recent report suggested that neutrophils are essential to stimulate auto-digestion (Sendler et al., 2013). The recruitment of neutrophils during pancreatic destruction in the zebrafish suggests that pancreatic disease observed in *cftr* mutants reflects early stages of pancreatitis and indicates that the *cftr* mutant pancreas may be a useful model to study the onset of pancreatitis. While these results suggest a role for neutrophils during pancreatic destruction, a definitive demonstration will require more

comprehensive and focused studies. It will also be important to investigate the role of macrophages in this process to gain a more complete understanding of the innate immune system in the CF pancreas. A better understanding of the precise mechanisms that lead to pancreatic destruction will be essential to preserving remaining pancreatic function in pancreatic sufficient CF patients and for pancreatitis promoted by single mutant CFTR alleles. A robust zebrafish genetic model of pancreatitis may facilitate discovery of new avenues for treatment and prevention of pancreatic destruction.

Recent reports indicate that CFTR also functions to regulate insulin secretion in the β cells of pancreatic islets (Guo et al., 2014). We found that the β cells develop normally in *cftr* mutants and, consistent with previous reports, we observed that islets in the adult pancreas were largely spared from destruction of the surrounding acinar cells. Further, we did not observe expression of *cftr* in the islet, although we cannot rule out the possibility that *cftr* is expressed in the islets at very low levels. While in vitro studies point to a role for *cftr* the pancreatic islet, it will be important to identify whether *cftr* is required for β cell function in vivo. Standard glucose tolerance tests are not simple to perform in the zebrafish, so it will be important to develop new tools for monitoring insulin secretion and electrical currents in the β cells to more specifically test whether *cftr* mutant zebrafish develop a form of CFRD.

The zebrafish represents a new model for screening for compounds and genes that modulate Cftr activity. Substantial effort has been allocated to identify compounds to treat CF by correcting or improving the activity of mutant CFTR alleles, especially the most common allele, CFTRΔF508. While several compounds have seen success in vitro, their efficacy has rarely translated to humans. A recent pair of studies investigating a combination of the two most promising compounds to treat CFTRΔF508 suggests that they may have antagonistic effects, limiting their efficacy (Cholon et al., 2014; Veit et al., 2014). These studies highlight the critical importance of identifying new compounds that are functional in vivo.

The zebrafish offers an in vivo model for rapidly assaying *cftr* activity. The zebrafish organ of left-right asymmetry, Kupffer's vesicle (KV), is an enclosed lumen inflated by Cftr-dependent fluid secretion (Navis et al., 2013). Loss of fluid secretion in *cftr* mutant zebrafish can be easily observed as a failure of KV lumen expansion at the 10–12 somite stage, occurring within 14 hours post fertilization (hpf) or as late at 24 hpf if the fish are grown at lower temperature. Additionally, drugs that modulate *cftr* activity regulate the size of Kupffer's vesicle, indicating that the organ can indicate Cftr activity level (Navis et al., 2013). Compounds that rescue activity of CFTRΔF508 expressed in the zebrafish Kupffer’s vesicle could represent a new class of therapeutics to more effectively treat CF in vivo.

A recent focus of the CF community has been to identify modifier genes of CF that influence disease outcome (Drumm et al., 2005). The zebrafish offers a new way to identify CF modifiers through forward genetic screens. A suppressor screen in the zebrafish could offer a new, unbiased approach to identify genes that modulate Cftr-dependent fluid secretion in Kupffer’s vesicle or prevent pancreatic pathology in *cftr* mutants. Forward genetic screens in the zebrafish may identify entirely new modifiers of CF to open new avenues for treatment.

The zebrafish has lacked robust transgenic markers of the pancreatic ducts. Here, we demonstrate that Cftr is a clear marker of the pancreatic duct in zebrafish. Transgenic lines that express C-terminal GFP or RFP fusions mark the apical membrane of the pancreatic duct throughout zebrafish life. Additionally, we generated a new line, *TgBAC(cftr:Gal4)*, which expresses Gal4 under the control of the *cftr* promoter. In combination with various UAS lines, *cftr:Gal4* can drive a variety of functional reagents in the pancreatic duct. These markers of *cftr* expression will allow new analysis of pancreatic duct development and function.

Conclusions

This study describes a new model for understanding the onset and pathophysiology of cystic fibrosis in the pancreas and other organs. We identified that *cftr* is a clear marker of the zebrafish pancreatic duct in vivo using several transgenic lines and that loss of Cftr function mirrors many aspects of CF. We were unable to identify early defects in the development of the pancreas, suggesting that *cftr* is instead essential for function of the pancreatic ducts in the larval and adult zebrafish. Importantly, we demonstrate that the zebrafish undergoes severe pancreatic destruction reminiscent of CF in humans. The zebrafish is a powerful genetic model with clear readouts of Cftr activity that will simplify in vivo pharmacological and genetic screens. Furthermore, the rapid onset of pancreatitis in the *cftr* mutant zebrafish offers a robust genetic model to study mechanisms driving pancreatitis. This work establishes *cftr* mutant zebrafish as a model of pancreatic disease similar to that of human CF.

Supplementary Material

Refer to Web version on PubMed Central for supplementary material.

Acknowledgments

We thank members of the Bagnat lab for helpful discussions and critical review throughout the project; Jennifer Moss for a generous gift of the CP-A antibody; James Norman for assistance analyzing fish survival; Allison Navis for assistance with histology; Mike Parsons and Duc Dong for providing the *TgBAC(ptf1a:Gal4)* and *Tg(ptf1a:GFP)* lines; Jennifer Moss, John Rawls, and Didier Stainier for critical reading of this manuscript.

Funding

This work was supported by a National Institutes of Health (NIH) innovator grant, DP2OD006486, to M.B.

References

Abu-El-Haija M, Ramachandran S, Meyerholz DK, Abu-El-Haija M, Griffin M, Giriyappa RL, Stoltz DA, Welsh MJ, McCray PB, Uc A. Pancreatic damage in fetal and newborn cystic fibrosis pigs involves the activation of inflammatory and remodeling pathways. Am. J. Pathol. 2012; 181:499–507. [PubMed: 22683312]

Alvers AL, Ryan S, Scherz PJ, Huisken J, Bagnat M. Single continuous lumen formation in the zebrafish gut is mediated by smoothened-dependent tissue remodeling. Development (Cambridge, England). 2014; 141:1110–1119.

Ameen NA, Ardito T, Kashgarian M, Marino CR. A unique subset of rat and human intestinal villus cells express the cystic fibrosis transmembrane conductance regulator. Gastroenterology. 1995; 108:1016–1023. [PubMed: 7535272]

Andersen DH. Cystic fibrosis of the pancreas and its relation to celiac disease: a clinical and pathological study. Am J Dis Child. 1938; 56:344–399.

Anderson MP, Gregory RJ, Thompson S, Souza DW, Paul S, Mulligan RC, Smith, CF of the zebrafish pancreas/13 AE, Welsh MJ. Demonstration that CFTR is a chloride channel by alteration of its anion selectivity. Science (New York, NY). 1991; 253:202–205.

Asakawa K, Suster ML, Mizusawa K, Nagayoshi S, Kotani T, Urasaki A, Kishimoto Y, Hibi M, Kawakami K. Genetic dissection of neural circuits by Tol2 transposon-mediated Gal4 gene and enhancer trapping in zebrafish. Proc Natl Acad Sci USA. 2008; 105:1255–1260. [PubMed: 18202183]

Bagnat M, Cheung ID, Mostov KE, Stainier DYR. Genetic control of single lumen formation in the zebrafish gut. Nat Cell Biol. 2007; 9:954–960. [PubMed: 17632505]

Bagnat M, Navis A, Herbstreith S, Brand-Arzamendi K, Curado S, Gabriel S, Mostov KE, Huisken J, Stainier DYR. Cse1l is a negative regulator of CFTR-dependent fluid secretion. Curr Biol. 2010; 20:1840–1845. [PubMed: 20933420]

Barrett KE, Keely SJ. Chloride secretion by the intestinal epithelium: molecular basis and regulatory aspects. Annu Rev Physiol. 2000; 62:535–572. [PubMed: 10845102]

Boom A, Lybaert P, Pollet J-F, Jacobs P, Jijakli H, Golstein PE, Sener A, Malaisse WJ, Beauwens R. Expression and localization of cystic fibrosis transmembrane conductance regulator in the rat endocrine pancreas. Endocrine. 2007; 32:197–205. [PubMed: 18040894]

Cartwright JHE, Piro O, Tuval I. Fluid dynamics in developmental biology: moving fluids that shape ontogeny. Hfsp J. 2009; 3:77–93. [PubMed: 19794816]

Cholon DM, Quinney NL, Fulcher ML, Esther CR, Das J, Dokholyan NV, Randell SH, Boucher RC, Gentzsch M. Potentiator ivacaftor abrogates pharmacological correction of ΔF508 CFTR in cystic fibrosis. Sci Transl Med. 2014; 6:246ra96.

Cohn JA, Friedman KJ, Noone PG, Knowles MR, Silverman LM, Jowell PS. Relation between mutations of the cystic fibrosis gene and idiopathic pancreatitis. New England Journal of Medicine. 1998; 339:653–658. [PubMed: 9725922]

Cohn JA, Strong TV, Picciotto MR, Nairn AC, Collins FS, Fitz JG. Localization of the cystic fibrosis transmembrane conductance regulator in human bile duct epithelial cells. Gastroenterology. 1993; 105:1857–1864. [PubMed: 7504645]

Crossley JR, Elliott RB, Smith PA. Dried-blood spot screening for cystic fibrosis in the newborn. Lancet. 1979; 1:472–474. [PubMed: 85057]

DiMagno EP, Go VL, Summerskill WH. Relations between pancreatic enzyme ouputs and malabsorption in severe pancreatic insufficiency. New England Journal of Medicine. 1973; 288:813–815. [PubMed: 4693931]

Dong PDS, Munson CA, Norton W, Crosnier C, Pan X, Gong Z, Neumann CJ, Stainier DYR. Fgf10 regulates hepatopancreatic ductal system patterning and differentiation. Nat Genet. 2007; 39:397–402. [PubMed: 17259985]

Dorin JR, Dickinson P, Alton EW, Smith SN, Geddes DM, Stevenson BJ, Kimber WL, Fleming S, Clarke AR, Hooper ML. Cystic fibrosis in the mouse by targeted insertional mutagenesis. Nature. 1992; 359:211–215. [PubMed: 1382232]

Drumm ML, Konstan MW, Schluchter MD, Handler A, Pace R, Zou F, Zariwala M, Fargo D, Xu A, Dunn JM, Darrah RJ, Dorfman R, Sandford AJ, Corey M, Zielenski J, Durie P, Goddard K, Yankaskas JR, Wright FA, Knowles MR. Genetic Modifiers of Lung Disease in Cystic Fibrosis. N Engl J Med. 2005; 353:1443–1453. [PubMed: 16207846]

Durie PR, Forstner GG. Pathophysiology of the exocrine pancreas in cystic fibrosis. J R Soc Med. 1989; 82(Suppl 16):2–10. [PubMed: 2657051]

Durie PR, Kent G, Phillips MJ, Ackerley CA. Characteristic multiorgan pathology of cystic fibrosis in a long-living cystic fibrosis transmembrane regulator knockout murine model. Am. J. Pathol. 2004; 164:1481–1493. [PubMed: 15039235]

Durno C, Corey M, Zielenski J, Tullis E, Tsui L-C, Durie P. Genotype and phenotype correlations in patients with cystic fibrosis and pancreatitis. Gastroenterology. 2002; 123:1857–1864. [PubMed: 12454843]

Fallon MB, Gorelick FS, Anderson JM, Mennone A, Saluja A, Steer ML. Effect of cerulein hyperstimulation on the paracellular barrier of rat exocrine pancreas. Gastroenterology. 1995; 108:1863–1872. [PubMed: 7539388]

Farooq M, Sulochana KN, Pan X, To J, Sheng D, Gong Z, Ge R. Histone deacetylase 3 (hdac3) is specifically required for liver development in zebrafish. Developmental Biology. 2008; 317:336–353. [PubMed: 18367159]

Gaskin KJ, Waters DL, Howman-Giles R, de Silva M, Earl JW, Martin HC, Kan AE, Brown JM, Dorney SF. Liver disease and common-bile-duct stenosis in cystic fibrosis. New England Journal of Medicine. 1988; 318:340–346. [PubMed: 3340104]

Godinho L, Mumm JS, Williams PR, Schroeter EH, Koerber A, Park SW, Leach SD, Wong ROL. Targeting of amacrine cell neurites to appropriate synaptic laminae in the developing zebrafish retina. Development (Cambridge, England). 2005; 132:5069–5079.

Guo JH, Chen H, Ruan YC, Zhang XL, Zhang XH, Fok KL, Tsang LL, Yu MK, Huang WQ, Sun X, Chung YW, Jiang X, Sohma Y, Chan HC. Glucose-induced electrical activities and insulin secretion in pancreatic islet β-cells are modulated by CFTR. Nat Commun. 2014; 5(4420)

Hall C, Flores MV, Storm T, Crosier K, Crosier P. The zebrafish lysozyme C promoter drives myeloid-specific expression in transgenic fish. BMC Developmental Biology. 2007; 5(2):7, 42. 2005.

Handwerger S, Roth J, Gorden P, Di Sant' Agnese P, Carpenter DF, Peter G. Glucose intolerance in cystic fibrosis. New England Journal of Medicine. 1969; 281:451–461. [PubMed: 4894429]

Hodges CA, Grady BR, Mishra K, Cotton CU, Drumm ML. Cystic fibrosis growth retardation is not correlated with loss of Cftr in the intestinal epithelium. AJP: Gastrointestinal and Liver Physiology. 2011; 301:G528–G536.

Iannucci A, Mukai K, Johnson D, Burke B. Endocrine pancreas in cystic fibrosis: an immunohistochemical study. Hum pathol. 1984; 15:278–284. [PubMed: 6365738]

Kemppainen E, Hedström J, Puolakkainen P, Halttunen J, Sainio V, Haapiainen R, Kivilaakso E, Stenman UH. Increased serum trypsinogen 2 and trypsin 2-alpha 1 antitrypsin complex values identify endoscopic retrograde cholangiopancreatography induced pancreatitis with high accuracy. Gut. 1997; 41:690–695. [PubMed: 9414980]

Kesavan G, Sand FW, Greiner TU, Johansson JK, Kobberup S, Wu X, Brakebusch C, Semb H. Cdc42-mediated tubulogenesis controls cell specification. Cell. 2009; 139:791–801. [PubMed: 19914171]

Kramer-Zucker AG, Olale F, Haycraft CJ, Yoder BK, Schier AF, Drummond IA. Cilia-driven fluid flow in the zebrafish pronephros, brain and Kupffer's vesicle is required for normal organogenesis. Development (Cambridge, England). 2005; 132:1907–1921.

Lerch MM, Gorelick FS. Models of Acute and Chronic Pancreatitis. Gastroenterology. 2013; 144:1180–1193. [PubMed: 23622127]

Lowery LA, Sive H. Initial formation of zebrafish brain ventricles occurs independently of circulation and requires the nagie oko and snakehead/atp1a1a.1 gene products. Development (Cambridge, England). 2005; 132:2057–2067.

Löhr M, Goertchen P, Nizze H, Gould NS, Gould VE, Oberholzer M, Heitz PU, Klöppel G. Cystic fibrosis associated islet changes may provide a basis for diabetes. An immunocytochemical and morphometrical study. Virchows Arch A Pathol Anat Histopathol. 1989; 414:179–185. [PubMed: 2492695]

Mackie ADR, Thornton SJ, Edenborough FP. Cystic fibrosis-related diabetes. Diabet. Med. 2003; 20:425–436. [PubMed: 12786675]

Matsui H, Grubb BR, Tarran R, Randell SH, Gatzy JT, Davis CW, Boucher RC. Evidence for periciliary liquid layer depletion, not abnormal ion composition, in the pathogenesis of cystic fibrosis airways disease. Cell. 1998; 95:1005–1015. [PubMed: 9875854]

Mayerle J, Schnekenburger J, Krüger B, Kellermann J, Ruthenbürger M, Weiss FU, Nalli A, Domschke W, Lerch MM. Extracellular cleavage of E-cadherin by leukocyte elastase during acute experimental pancreatitis in rats. Gastroenterology. 2005; 129:1251–1267. [PubMed: 16230078]

Meyerholz DK, Stoltz DA, Pezzulo AA, Welsh MJ. Pathology of gastrointestinal organs in a porcine model of cystic fibrosis. Am. J. Pathol. 2010; 176:1377–1389. [PubMed: 20110417]

Moss JB, Koustubhan P, Greenman M, Layer R, Walter I, Moss LG. Regeneration of the Pancreas in Adult Zebrafish. Diabetes. 2009; 58:1844–1851. [PubMed: 19491207]

Navis A, Marjoram L, Bagnat M. Cftr controls lumen expansion and function of Kupffer's vesicle in zebrafish. Development (Cambridge, England). 2013; 140:1703–1712.

Nedvetsky PI, Emmerson E, Finley JK, Ettinger A, Cruz-Pacheco N, Prochazka J, Haddox CL, Northrup E, Hodges C, Mostov KE, Hoffman MP, Knox SM. Parasympathetic innervation regulates tubulogenesis in the developing salivary gland. Dev Cell. 2014; 30:449–462. [PubMed: 25158854]

Olivier AK, Yi Y, Sun X, Sui H, Liang B, Hu S, Xie W, Fisher JT, Keiser NW, Lei D, Zhou W, Yan Z, Li G, Evans TIA, Meyerholz DK, Wang K, Stewart ZA, Norris AW, Engelhardt JF. Abnormal endocrine pancreas function at birth in cystic fibrosis ferrets. J Clin Invest. 2012; 122:3755–3768. [PubMed: 22996690]

Ostedgaard LS, Meyerholz DK, Chen J-H, Pezzulo AA, Karp PH, Rokhlina T, Ernst SE, Hanfland RA, Reznikov LR, Ludwig PS, Rogan MP, Davis GJ, Dohrn CL, Wohlford-Lenane C, Taft PJ, Rector MV, Hornick E, Nassar BS, Samuel M, Zhang Y, Richter SS, Uc A, Shilyansky J, Prather RS, McCray PB, Zabner J, Welsh MJ, Stoltz DA. The ΔF508 mutation causes CFTR misprocessing and cystic fibrosis-like disease in pigs. Sci Transl Med. 2011; 3:74ra24.

Parsons MJ, Pisharath H, Yusuff S, Moore JC, Siekmann AF, Lawson ND, Leach SD. Notch-responsive cells initiate the secondary transition in larval zebrafish pancreas. Mechanisms of Development. 2009; 126:898–912. [PubMed: 19595765]

Pauls S, Zecchin E, Tiso N, Bortolussi M, Argenton F. Function and regulation of zebrafish nkx2.2a during development of pancreatic islet and ducts. Developmental Biology. 2007; 304:875–890. [PubMed: 17335795]

Phillips JB, Westerfield M. Zebrafish models in translational research: tipping the scales toward advancements in human health. Dis Model Mech. 2014; 7:739–743. [PubMed: 24973743]

Quinton PM. Cystic fibrosis: impaired bicarbonate secretion and mucoviscidosis. Lancet. 2008; 372:415–417. [PubMed: 18675692]

Riordan JR, Rommens JM, Kerem B, Alon N, Rozmahel R, Grzelczak Z, Zielenski J, Lok S, Plavsic N, Chou JL. Identification of the cystic fibrosis gene: cloning and characterization of complementary DNA. Science (New York, NY). 1989; 245:1066–1073.

Rock JR, O'Neal WK, Gabriel SE, Randell SH, Harfe BD, Boucher RC, Grubb BR. Transmembrane protein 16A (TMEM16A) is a Ca2+-regulated Cl− secretory channel in mouse airways. J Biol Chem. 2009; 284:14875–14880. [PubMed: 19363029]

Rogers CS, Stoltz DA, Meyerholz DK, Ostedgaard LS, Rokhlina T, Taft PJ, Rogan MP, Pezzulo AA, Karp PH, Itani OA, Kabel AC, Wohlford-Lenane CL, Davis GJ, Hanfland RA, Smith TL, Samuel M, Wax D, Murphy CN, Rieke A, Whitworth K, Uc A, Starner TD, Brogden KA, Shilyansky J, McCray PB, Zabner J, Prather RS, Welsh MJ. Disruption of the CFTR Gene Produces a Model of Cystic Fibrosis in Newborn Pigs. Science (New York, NY). 2008; 321:1837–1841.

Sendler M, Dummer A, Weiss FU, Krüger B, Wartmann T, Scharffetter-Kochanek K, van Rooijen N, Malla SR, Aghdassi A, Halangk W, Lerch MM, Mayerle J. Tumour necrosis factor α secretion induces protease activation and acinar cell necrosis in acute experimental pancreatitis in mice. Gut. 2013; 62:430–439. [PubMed: 22490516]

Sharer N, Schwarz M, Malone G, Howarth A, Painter J, Super M, Braganza J. Mutations of the cystic fibrosis gene in patients with chronic pancreatitis. New England Journal of Medicine. 1998; 339:645–652. [PubMed: 9725921]

Snelson CD, Santhakumar K, Halpern ME, Gamse JT. Tbx2b is required for the development of the parapineal organ. Development (Cambridge, England). 2008; 135:1693–1702.

Snouwaert JN, Brigman KK, Latour AM, Malouf NN, Boucher RC, Smithies O, Koller BH. An animal model for cystic fibrosis made by gene targeting. Science (New York, NY). 1992; 257:1083–1088.

Sturgess JM. Structural and developmental abnormalities of the exocrine pancreas in cystic fibrosis. J. Pediatr. Gastroenterol. Nutr. 1984; 3(Suppl 1):S55–S66. [PubMed: 6502395]

Sun X, Sui H, Fisher JT, Yan Z, Liu X, Cho H-J, Joo NS, Zhang Y, Zhou W, Yi Y, Kinyon JM, Lei-Butters DC, Griffin MA, Naumann P, Luo M, Ascher J, Wang K, Frana T, Wine JJ, Meyerholz

DK, Engelhardt JF. Disease phenotype of a ferret CFTR-knockout model of cystic fibrosis. J Clin Invest. 2010; 120:3149–3160. [PubMed: 20739752]

Sun X, Yan Z, Yi Y, Li Z, Lei D, Rogers CS, Chen J, Zhang Y, Welsh MJ, Leno GH, Engelhardt JF. Adeno-associated virus-targeted disruption of the CFTR gene in cloned ferrets. J Clin Invest. 2008; 118:1578–1583. [PubMed: 18324338]

Suster ML, Kikuta H, Urasaki A, Asakawa K, Kawakami K. Transgenesis in zebrafish with the tol2 transposon system. Methods Mol Biol. 2009; 561:41–63. [PubMed: 19504063]

Veit G, Avramescu RG, Perdomo D, Phuan P-W, Bagdány M, Apaja PM, Borot F, Szollosi D, Wu Y-S, Finkbeiner WE, Hegedus T, Verkman AS, Lukacs GL. Some gating potentiators, including VX-770, diminish ΔF508-CFTR functional expression. Sci Transl Med. 2014; 6:246ra97–246ra97.

Wan Y, Otsuna H, Chien C-B, Hansen C. FluoRender: An Application of 2D Image Space Methods for 3D and 4D Confocal Microscopy Data Visualization in Neurobiology Research. IEEE Pac Vis Symp. 2012:201–208. [PubMed: 23584131]

Wang X, Robertson AL, Li J, Chai RJ, Haishan W, Sadiku P, Ogryzko NV, Everett M, Yoganathan K, Luo HR, Renshaw SA, Ingham PW. Inhibitors of neutrophil recruitment identified using transgenic zebrafish to screen a natural product library. Dis Model Mech. 2014; 7:163–169. [PubMed: 24291762]

Warming S, Costantino N, Court DL, Jenkins NA, Copeland NG. Simple and highly efficient BAC recombineering using galK selection. Nucleic Acids Res. 2005; 33:e36. [PubMed: 15731329]

Westerfield, M. The zebrafish book: a guide for the laboratory use of zebrafish (Danio rerio). University of Oregon Press; 2000.

Whitcomb DC. Mechanisms of disease: Advances in understanding the mechanisms leading to chronic pancreatitis. Nat Clin Pract Gastroenterol Hepatol. 2004; 1:46–52. [PubMed: 16265044]

Wilschanski M, Novak I. The cystic fibrosis of exocrine pancreas. Cold Spring Harb Perspect Med. 2013; 3:a009746–a009746. [PubMed: 23637307]

Yang C-T, Cambier CJ, Davis JM, Hall CJ, Crosier PS, Ramakrishnan L. Neutrophils exert protection in the early tuberculous granuloma by oxidative killing of mycobacteria phagocytosed from infected macrophages. Cell Host Microbe. 2012; 12:301–312. [PubMed: 22980327]

Yee NS, Lorent K, Pack M. Exocrine pancreas development in zebrafish. Developmental Biology. 2005; 284:84–101. [PubMed: 15963491]

Highlights

- We characterize a cftr mutant zebrafish as a new model system for cystic fibrosis.
- We describe new transgenic lines for visualizing the pancreatic duct using cftr expression and localization.
- Zebrafish mutant for cftr undergo severe destruction of pancreatic acinar tissue.

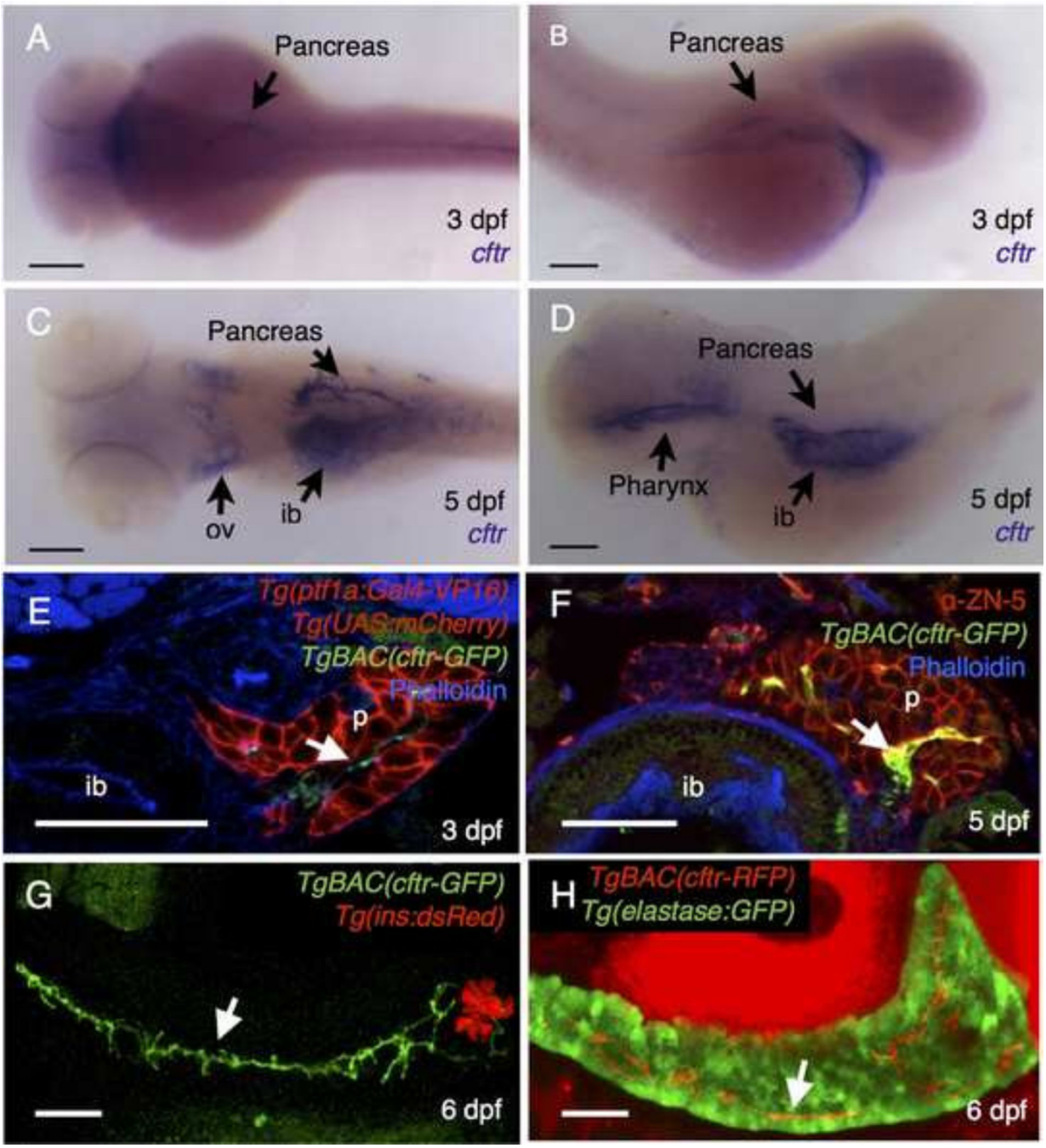

Figure 1. *cftr* is expressed in the pancreatic duct

(A–D) Wholemount in situ hybridization for *cftr*. (A) Dorsal and (B) lateral view of *cftr* expression at 3 dpf. (C) Dorsal and (D) lateral view of cftr expression at 5 dpf. (E,F) Transverse section of *TgBAC(cftr-GFP)* expressed in the pancreatic duct at (E) 3 dpf in conjunction with *ptf1a* expression in the acinar cells of the pancreas and (F) at 5 dpf in conjunction with ZN-5, an antibody that marks the pancreas. (G) Live, confocal image of *TgBAC(cftr-GFP)* expression along the length of the pancreatic duct in conjunction with *Tg(ins:dsRed)* to mark the β cells of the principal islet at 5 dpf. (H) Live confocal image of

ductal *TgBAC(cftr-RFP)* expression in conjunction with *ela:GFP* to indicate the acinar tissue. White arrows indicate *cftr* expression in the pancreatic duct. ib: intestinal bulb, ov: otic vesicle, p: pancreas. (A–D) Scale bars = 100 μm, (E–H) Scale bars = 50 μm.

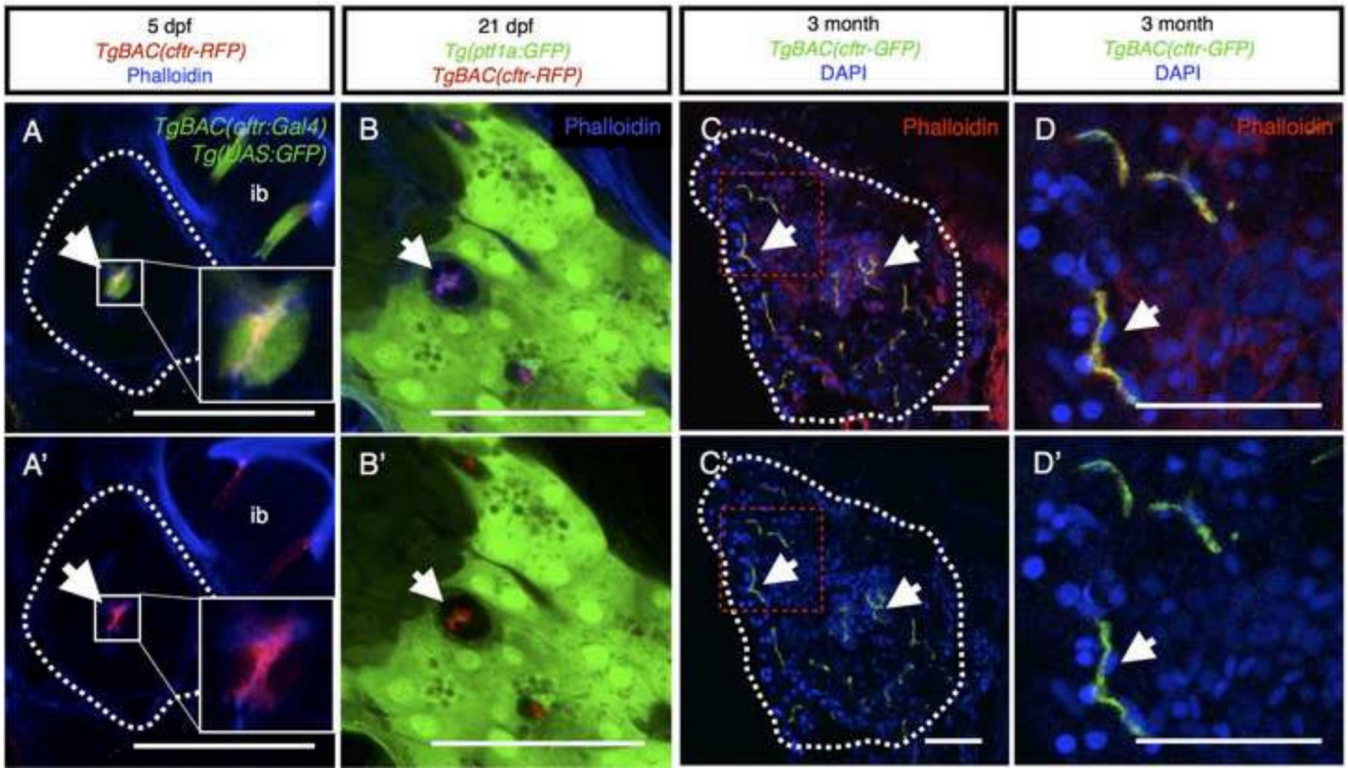

Figure 2. Cftr is localized to the apical membrane of the pancreatic duct epithelium throughout life

(A,A') Transverse section of 5 dpf larvae expressing *TgBAC(cftr-RFP)* to show Cftr-RFP localization and *TgBAC(cftr:Gal4); Tg(UAS:GFP)* to mark the cytosol of *cftr* expressing cells with GFP. Dashed white lines indicate the periphery of pancreas. Inset is 3× magnification of ductal cells. ib: intestinal bulb. (B,B') Transverse section of a 21 dpf larvae demonstrating Cftr-RFP localization at the apical membrane of the pancreatic duct in conjunction with *TgBAC(ptf1a-GFP)* expressed in the acinar cells. Cftr is observed at or near the apical membrane marked with phalloidin. (C,C') Transverse section of 3 month, adult pancreas indicating Cftr-GFP expression in pancreatic ducts throughout the pancreas. Dashed white lines indicate the periphery of the pancreas. Red dashed box indicates inset (D). (D,D') Cftr-GFP is localized at or near the apical membrane of the pancreatic ducts, marked by phalloidin staining. Arrows indicate ductal expression of Cftr. Scale bars = 50 μm.

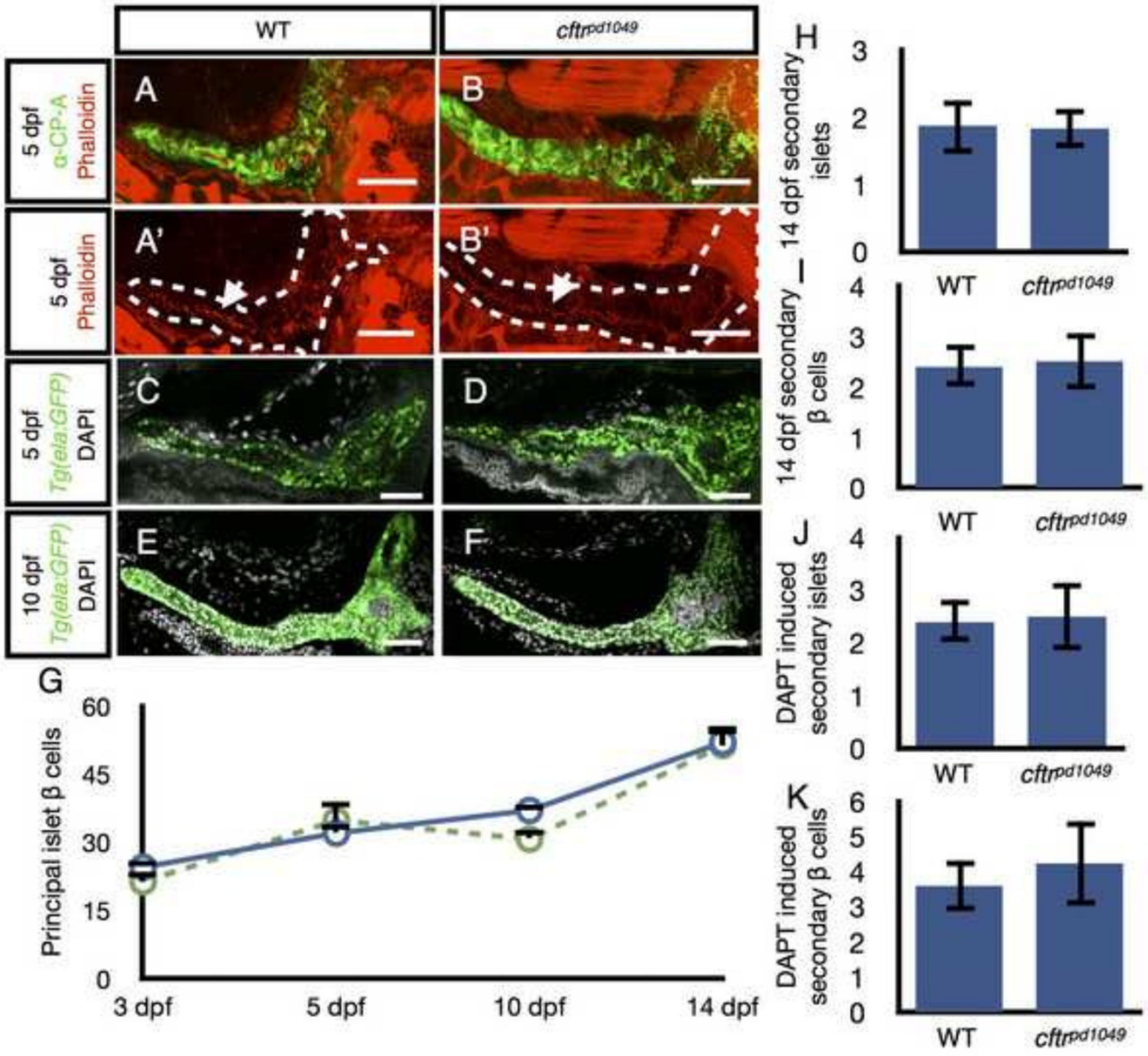

Figure 3. Development of the *cftr* mutant pancreas

(A) Wholemount confocal image of WT pancreas stained with anti-carboxypeptidase (CP-A) to detect acinar cells and phalloidin to mark actin at the apical membrane of the pancreatic duct. (A') Associated WT image without anti-CP-A to better visualize the contiguous actin strip along the length of the duct indicative of a continuous lumen. (B) Wholemount confocal image of a *cftr* pancreas stained with anti-CP-A and phalloidin. The actin network is contiguous in *cftr* mutants indicative of a continuous lumen. (C–F) Wholemount WT and *cftr* mutant samples expressing *ela:GFP* to mark acinar tissue and stained with DAPI to mark nuclei at (C,D) 5 dpf and (E,F) 10 dpf. (G) Quantification of principal islet β cells at several stages. (H) Quantification of total number of secondary islets at 14 dpf and (I) total number of secondary β cells at 14 dpf. WT, *n*=7; *cftr*^{pd1049} *n*=6. (J)

Quantification of DAPT induced secondary islets and (K) total number of DAPT induced secondary islet β cells. WT, *n*=5; *cftr*^{pd1049}, *n*=4. Error bars represent s.e.m. Scale bars = 50 μm.

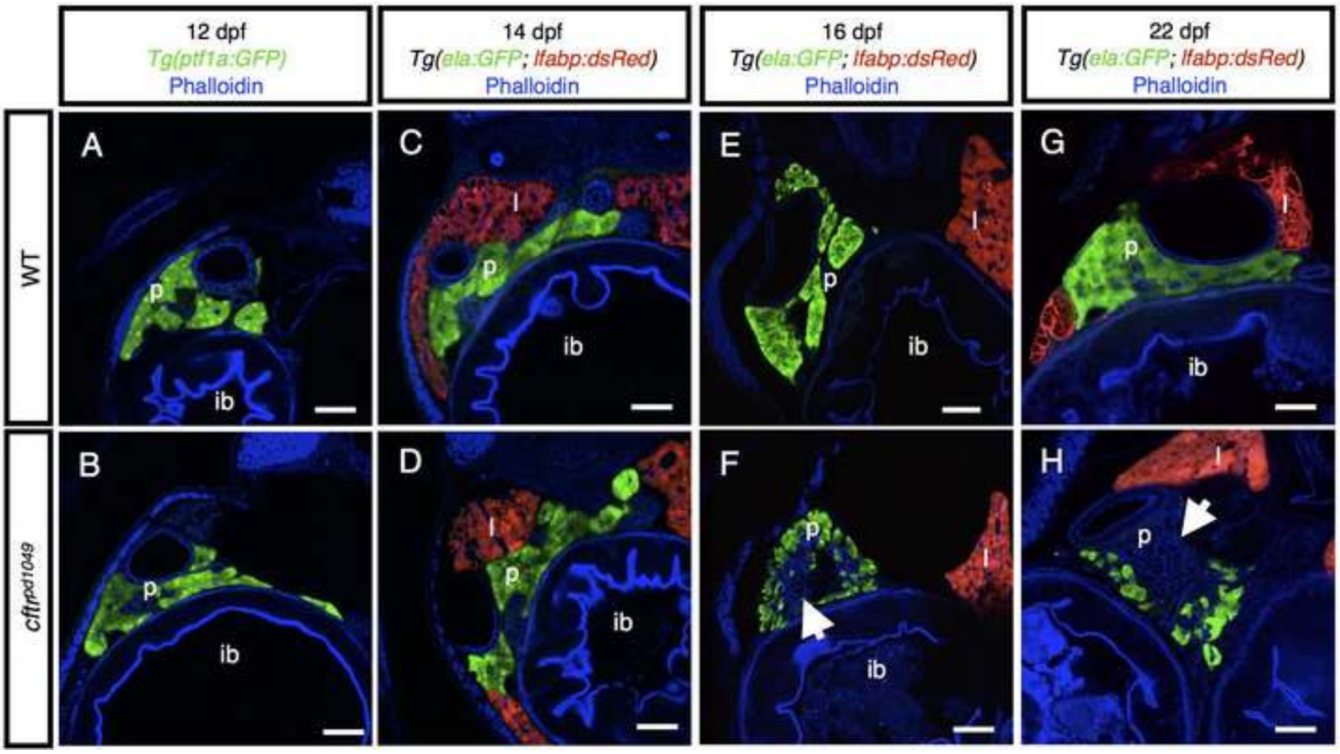

Figure 4. Timecourse of pancreatic destruction in *cftr* mutants

(A,B) Transverse section of *Tg(ptf1a:GFP)* expression marking the acinar cells in (A) WT and (B) *cftr* mutant samples. (C,D) Transverse section at 14 dpf of (C) WT and (D) *cftr* mutant pancreas marked by *ela:GFP* expression. (E,F) Transverse section of (E) WT and (F) *cftr* mutant samples expressing *ela:GFP* in the acini demonstrating loss of pancreatic acinar tissue at 16 dpf. (G,H) Transverse section of (G) WT and (H) *cftr* mutant samples expressing *ela:GFP* in the pancreas at 22 dpf with severe pancreatic destruction. Arrow indicates absent acinar tissue. Scale bars = 50 μm.

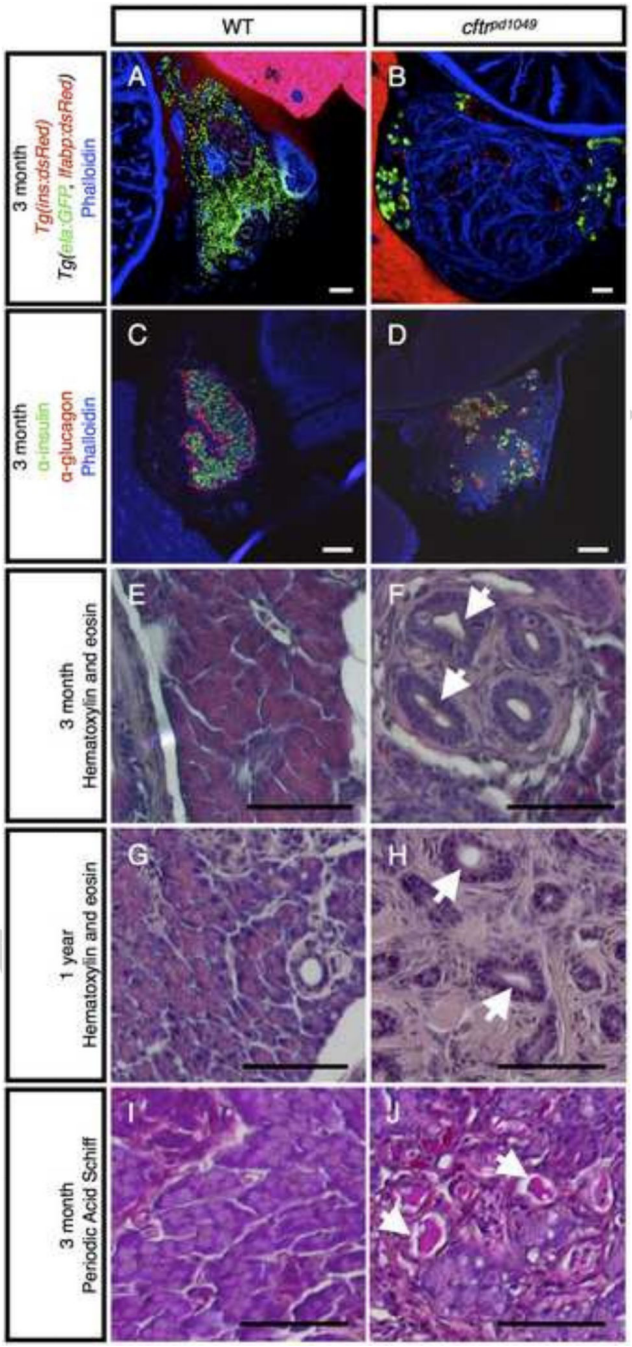

Figure 5. Adult *cftr* mutants undergo severe pancreatic destruction

(A,B) Transverse section of (A) WT and (B) *cftr*^{pd1049} mutant pancreas expressing *ela:GFP* in acinar cells. (C,D) Transverse section of 3 month post fertilization (mpf) WT and *cftr* mutant pancreas stained for insulin and glucagon to mark the pancreatic islets. (E–H) Hematoxylin and eosin staining of WT and *cftr* mutant pancreatic sections at (E,F) 3 mpf and (G,H) 1 year post fertilization. (I,J) Period Acid Schiff staining of 3 mpf transverse sections of the pancreas indicating mucus within the lumen of the pancreatic duct. Arrows indicate dilated pancreatic ducts. ib: intestinal bulb, p: pancreas, l: liver. Scale bars = 50 μm.

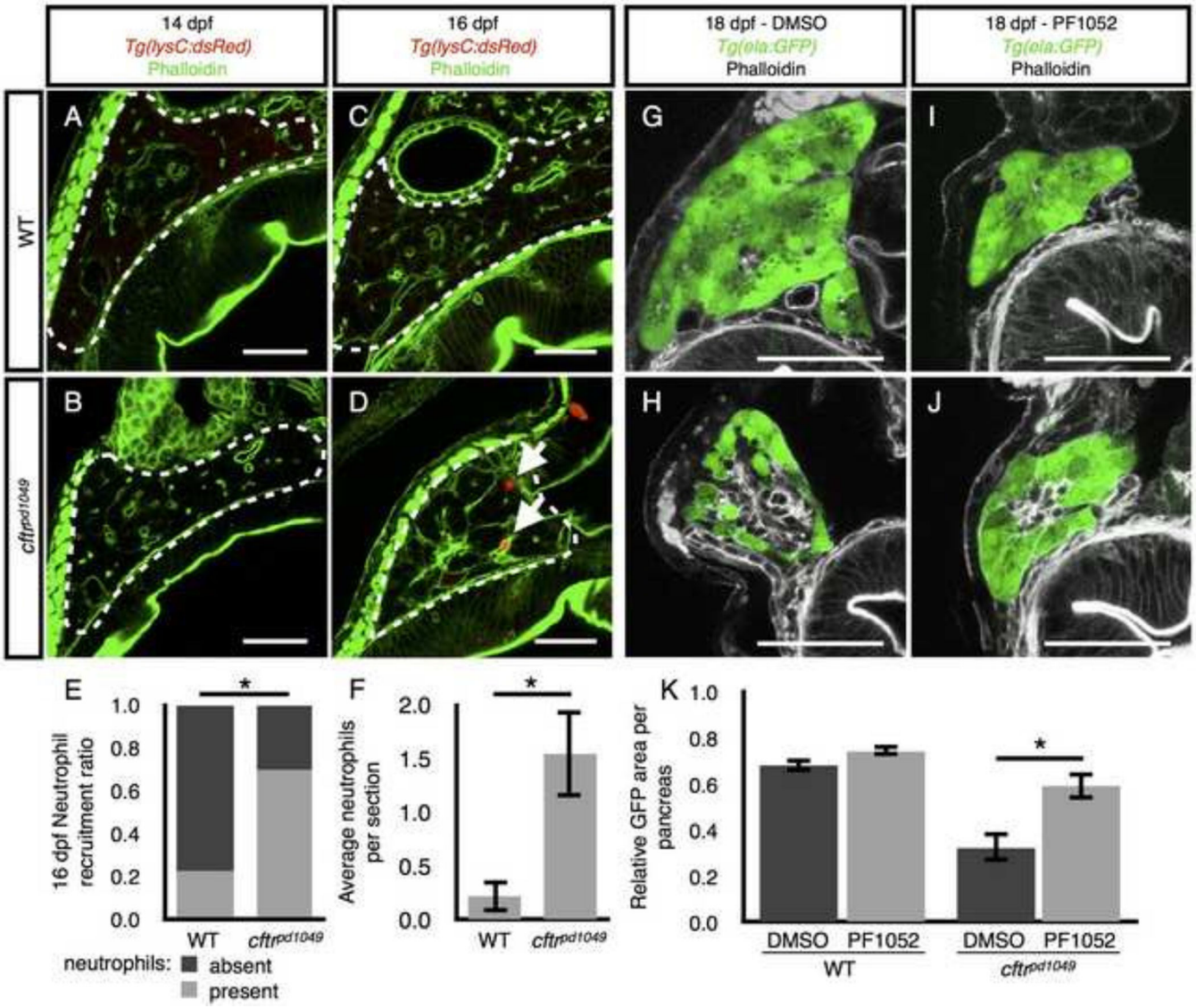

Figure 6. Neutrophil recruitment during pancreatic destruction

(A,B) Neutrophils are absent from representative sections of (A) WT and (B) *cftr* mutant pancreata at 14 dpf. (C,D) Neutrophils are absent from the (C) WT pancreas at 16 dpf, but present in the (D) *cftr* mutant pancreas. (E,F) Quantification of (E) the ratio of sections with neutrophils present versus absent to the total number of sections and (F) the average number of neutrophils observed in each pancreas indicating a significant difference in pancreatic neutrophils in the 16 dpf *cftr* mutant pancreas. The median number of neutrophils in each WT pancreas was 0, ranging from 0 to 1 and $cftr^{pd1049}$ was 1, ranging from 0 to 5. WT, n=8; $cftr^{pd1049}$, n=13; *P<0.01. Error bars represent s.e.m. (G,H) DMSO treated (G) WT and (H) *cftr* mutant samples at 18 dpf expressing *ela:GFP* in the acinar cells demonstrate typical pancreatic destruction. (I,J) Representative sections of (I) WT and (J) *cftr* mutant pancreata at 18 dpf treated with PF1052 showing preservation of acinar tissue. (K) Quantification of area of GFP expression divided by total pancreas area for each treatment group showings significantly more area of acinar tissue marked by *ela:GFP* in PF1052 treated mutants

compared with DMSO treated mutants. WT DMSO, *n*=8; WT PF1052, *n*=7; *cftr*^{pd1049} DMSO, *n*=8; *cftr*^{pd1049}, *n*=12; **P*<0.01. Error bars represent s.e.m. Arrows indicate neutrophils. Scale bars = 50 μm.